Local Thermodynamical Equilibrium and the Equation of State of Hot, Dense Matter Created in Au+Au Collisions at AGS

L.V. Bravina[a,1,2], M.I. Gorenstein[a,b,3], M. Belkacem[a,1], S.A. Bass[c,4], M. Bleicher[a], M. Brandstetter[a], M. Hofmann[a], S. Soff[a,d], C. Spieles[e,4], H. Weber[a], H. Stöcker[a] and W. Greiner[a]

[a] *Institut für Theoretische Physik, Goethe Universität Frankfurt, Germany*
[b] *School of Physics and Astronomy, Tel Aviv University, Tel Aviv, Israel*
[c] *Dept. of Physics, Duke University, Durham, USA*
[d] *Gesellschaft für Schwerionenforschung, Darmstadt, Germany*
[e] *Nuclear Science Division, LBNL, Berkeley, CA 94720, USA*
[1] *Alexander von Humboldt Foundation Fellow*
[2] *on leave of absence from the Institute for Nuclear Physics, Moscow State University, Russia*
[3] *Permanent address: Bogolyubov Institute for Theoretical Physics, Kiev, Ukraine*
[4] *Feodor Lynen Fellow of the Alexander von Humboldt Foundation*

Abstract

Local kinetic and chemical equilibration is studied for Au+Au collisions at 10.7 AGeV in the microscopic Ultrarelativistic Quantum Molecular Dynamics model (UrQMD). The UrQMD model exhibits dramatic deviations from equilibrium during the high density phase of the collision. Thermal and chemical equilibration of the hadronic matter seems to be established in the later stages during a quasi-isentropic expansion, observed in the central reaction cell with volume 125 fm^3. For $t \geq$10 fm/c the hadron energy spectra in the cell are nicely reproduced by Boltzmann distributions with a common rapidly dropping temperature. Hadron yields change drastically and at the late expansion stage follow closely those of an ideal gas statistical model. The equation of state seems to be simple at late times: $P \cong 0.12\varepsilon$. The time evolution of other thermodynamical variables in the cell is also presented.

Key words: Statistical model, equation of state, thermalization, Monte-Carlo model for relativistic heavy ion collisions.
PACS: 25.75, 24.10.Lx, 24.10.Pa, 64.30.

1 Introduction

The main goal of the relativistic heavy-ion experiments at Brookhaven and CERN is to study the properties, e.g. the equation of state (EoS), of strongly interacting hot and dense hadronic matter produced in the course of nuclear collisions. A question of great importance in these studies is to determine the EoS and whether local (LTE) or even global thermodynamical equilibrium is reached in the system or not. This is a crucial point for a large group of models, widely used for data analysis. Despite the long history of such investigations (e.g. [1–7]), this question remains still open.

One can try to check the assumption of LTE by analyzing the experimental particle number ratios and hadron momentum spectra (e.g. [8–11]). Due to the time duration of chemical (inelastic) and kinetic (elastic) freeze-out of the system in A+A collisions [12–15], the answer is not conclusive. In contrast to the microscopic approaches [16–20], macroscopic models like hydrodynamical [21–23] or thermal [7,9,10] models adopt LTE as ad hoc assumption, use the Equation of State [24] as a parametrization and apply usually an instantaneous freeze-out of hadrons, produced from many different space-time cells. The freeze-out conditions for these cells – temperatures, baryonic chemical potentials and collective velocities – are actually quite different and model dependent (see e.g. [11,15,25]). Also note that the experimental particle spectra in elementary e^+e^- and hadron-hadron collisions at high energies already look "thermalized" [25,26].

Because of these difficulties it is very promising to check the LTE and to extract the EoS at different stages of relativistic heavy ion reactions based on a detailed microscopic analysis. Here, we employ for a such analysis the microscopic Ultrarelativistic Quantum Molecular Dynamics model (UrQMD) [16].

2 Ultrarelativistic Quantum Molecular Dynamics

UrQMD is a N-body transport model designed for describing heavy ion collisions in the laboratory energy range from several MeV to several TeV per nucleon. The detailed presentation of UrQMD and underlying concepts together with a comparison with experimental data is now publically accessible [16]. The model treats binary elastic and inelastic hadronic collisions and many-body resonance decays. The inelastic collisions and decays are the only source for changing the chemical composition of the system, while elastic collisions change only the momentum distributions of the hadrons. Both processes drive the system towards thermodynamical equilibrium. However, the time scales

may be too short in heavy ion collisions for actually achieving LTE.

The UrQMD model is based on string and resonance excitation both in primary nucleon-nucleon collisions from projectile and target, some also in secondary hadronic collisions. There are 55 baryon and 32 meson states as discrete degrees of freedom in the model as well as their anti-particles and explicit isospin-projected states with masses up to 2.5 GeV. From 1.5 GeV the strings can be populated as continuous degrees of freedom. The experimental hadron cross sections and resonance decay widths are used when possible. At high energies a string mechanism is implemented to simulate soft hadronic interactions. Hadrons, produced through the string decays, have non-zero formation time which depends on the four-momentum of the particle. Newly produced particles cannot interact during their formation time. Leading hadrons (containing the constituent quarks) interact within their formation time, but with reduced cross sections, proportional to the number of original valence quarks. The Pauli principle is applied to BB collisions by blocking the final state if the outgoing phase space is occupied. No Bose effects for mesons are implemented in UrQMD.

3 UrQMD analysis of Au+Au collisions.

Now let us use the UrQMD model to explore to which extent LTE can be reached at least in a small cell around the origin of central (b=0 fm) Au+Au collisions at 10.7 AGeV. The formation of hot and dense hadronic matter is expected in this reaction, therefore the comparison of local system properties predicted by UrQMD with those of the ideal hadron gas looks promising.

For our analysis we consider a cubic cell of volume $V = 5 \times 5 \times 5$ fm^3 centered around the origin of center-of-mass of Au+Au system. The collective velocity of this cell is equal to zero because the system geometry gives no preferable direction for the collective motion. The cell size should be small enough to avoid collective flow (and streaming) and not to underestimate densities inside the cell. On the other hand it should be large enough to contain enough particles inside the cell, which guarantees reasonably small fluctuations of particle observables in the cell. From our analysis (see below) it appears that a cubic cell with a side of 5 fm satisfies simultaneously both above requirements for 200 Au+Au central collisions at AGS energy.

We start by analyzing the time evolution of different physical quantities in the Au+Au center-of-mass frame. Time $t = 0$ fm/c corresponds to the moment when the two Lorentz contracted nuclei touch each other. The maximum overlap of the nuclei occurs at about 2.5 fm/c. At time $t = 2R_{Au}/(\gamma_{cm} v_{cm}) \cong 5.5$ fm/c the freely streaming nuclei would have passed through each other.

The reaction is dominated by strong momentum anisotropies for all particles inside the cell. During the entire high energy density phase, t <10 fm/c, the widths of the velocity distributions in the longitudinal ($z-$)direction, σ_z, are much larger then the widths in the transverse ($x-$, $y-$) directions, σ_x and σ_y, for each hadron species. However, for $t \geq$10 fm/c the anisotropies inside the central cell disappear and the widths σ_i become approximately equal. The velocity component distributions of nucleons in the cell, shown in Fig. 1 at two different times, confirm this result. The shapes of the velocity distributions are very different for v_z and $v_\perp$ at t=5 fm/c. They become very similar at t=10 fm/c. This approximate isotropy of hadronic velocity distributions in the central cell appears to be due to the escape of fast or non-scattered particles from the cell and as a result of many hadronic rescatterings. At t =10 fm/c the newly produced particles in the cell have undergone from 1.5 (pions and $\bar{K}$) to 5 (K) elastic collisions, while the baryons have suffered more than 20 strong interactions. Fig. 2 shows the large difference between the hadrons containing original constituent quarks ($< n_{coll} > \cong 10 - 30$) and newly bred mesons ($< n_{coll} > \cong 1 - 3$). There are still some collisions in the cell at t >18 fm/c. Fig. 3 shows that for $t \leq$18 fm/c only a small fraction of the particles in the cell is frozen out before that time.

The isotropy of the momentum distributions for all hadron species in the cell is a necessary prerequisite for LTE. The next observation is that hadron energy spectra in the central cell at $t \geq$10 fm/c are nicely fitted by Boltzmann distributions, $\exp(-E_i/T)$, with rapidly falling $T-$values vs. time. At each moment, however, all particle species i exhibit practically the same slope. The "temperatures", T, agree to within $\Delta T \cong$10 MeV.

4 Ideal Gas Statistical Model.

To study chemical equilibrium in detail, let us now compare the hadron spectra and yields in the cell, as predicted by UrQMD model, with those of a Statistical Model of an ideal hadron gas (SM) [27,28]. For this comparison of the UrQMD results to the SM model the time interval from 10 to 18 fm/c is chosen. The largest values of the energy density, $\varepsilon \cong 21\varepsilon_0$, and baryonic density, $\rho_B \cong 10\rho_0$, in the central reaction zone are reached earlier, at $t \cong$4-5 fm/c. At this time, however, the system of particles in the cell is not yet thermalized and still exhibits strong velocity anisotropy. At $t \cong 4 - 5$ fm/c there is also a large fraction of non-formed and non-interacting particles in the cell, particularly mesons (see Fig. 3). Hence, the physical interpretation of this early stage of the reaction should - in the present approach - not be carried forward in a SM model. For $t \geq$10 fm/c the fraction of non-formed particles goes to zero rapidly. On the other hand the total number of particles in the cell is small at $t >$ 18 fm/c and the system approaches its thermal freeze-out (no collisions

occur) stage. In this paper we restrict our analysis of LTE to the time interval between t=10–18 fm/c. We do not discuss the "initial" stage with high energy density and the "final" kinetic stage of particle freeze-out.

For a thermalized ideal gas the momentum spectrum of particle species "i" in the rest frame of the cell can be presented as

$$\frac{dN_i}{d^3p} \;=\; \frac{g_i\,V}{(2\pi\hbar)^3}\;\exp\left(\frac{\mu_i}{T}\right)\;\exp\left(-\frac{E_i}{T}\right) \;\equiv\; \frac{g_i\,V}{(2\pi\hbar)^3}\;f_i\;, \qquad (1)$$

where V is the volume of the cell, T is the temperature of the system in the cell, g_i, m_i, $E_i = (p^2 + m_i^2)^{1/2}$ and μ_i are the degeneracy factor, the mass, the energy and the chemical potential of the hadron species "i", correspondingly. Here, Boltzmann distribution functions, f_i, are used for all hadrons. Quantum statistical effects are not included in the present analysis.

With the term thermodynamical equilibrium we specifically mean both kinetic and chemical equilibrium. The chemical potential of particle i in LTE can be represented as

$$\mu_i \;=\; b_i\mu_B \;+\; s_i\mu_S \qquad (2)$$

in terms of the baryonic-, μ_B, and strange-, μ_S, chemical potentials ($b_i = 0, \pm 1$, $s_i = 0, \mp 1, \mp 2, \mp 3$ are, respectively, the baryonic- and strange- charges of the particle species "i"). The electric chemical potential considered in [29,30] is neglected.

5 Results and discussion.

Here, 200 Au+Au events, generated with UrQMD, are analyzed using the following procedure. The average energy density, ε, baryonic density, ρ_B, and net strangeness density, ρ_S, in the cell are calculated for $10 \leq t \leq 18$ fm/c. The contributions of both formed and not yet formed particles are included. The values of ε, ρ_B and ρ_S are inserted in the l.h.s. of the following equations:

$$\varepsilon \;=\; \sum_i \varepsilon_i\;, \quad \rho_B \;=\; \sum_i b_i\;n_i\;, \quad \rho_S \;=\; \sum_i s_i\;n_i\;. \qquad (3)$$

Here

$$n_i \;=\; \frac{g_i}{2\pi^2\hbar^3}\int\limits_0^\infty p^2dp\;f_i\;, \quad \varepsilon_i \;=\; \frac{g_i}{2\pi^2\hbar^3}\int\limits_0^\infty p^2dp\;(p^2 \;+\; m_i^2)^{1/2}\;f_i$$

are the number- and energy density of particle species "i" predicted by the ideal gas model. The ideal gas model employs the same hadron species "i" as the UrQMD model. Solving the system of three equations (3) for the three unknown parameters, T, μ_B and μ_S, we find the results presented in Table 1.

5.1 Thermalization in central reaction zone.

Now we can turn to the predictions of the Statistical model (SM) for the specific single particle spectra, Eq. (1), by using the intensive parameters T, μ_B and μ_S, extracted from the average energy density, ε, baryon density, ρ_B, and strangeness density, ρ_S. Also the pressure and the entropy can be calculated swiftly (see below). The Boltzmann energy spectra Eq. (1) predicted by the SM with T, μ_B, μ_S values from Table 1 and the spectra obtained in the UrQMD model in the central cell for different particle species agree surprisingly well for all instants t between 10 and 18 fm/c. Fig. 4 shows this comparison for t=13 fm/c. Between 10 and 18 fm/c also the hadronic yields, obtained in the SM, are rather close to the UrQMD data, see Fig. 3. These results seem to indicate that the LTE is closely resembled for the hadronic matter in central cell of central Au+Au collisions at 10.7 AGeV at least for t =10 to 18 fm/c. The statistical model parameters, i.e. the main thermodynamic characteristics of the cell change rapidly with time. This clearly demonstrates that a fireball type description of hadronic matter is inadequate.

Table 1 shows that during this time interval (10 – 18 fm/c) the baryonic density and temperature in the cell change from $\rho_B \cong 2\rho_0$ to $0.3\rho_0$ ($\rho_0 = 0.16$ fm^{-3} is the normal nuclear density) and from $T \cong$150 MeV to 100 MeV. The time evolution of the central cell in (T, ρ_B-) plane is shown in Fig. 5. It resembles closely an isentropic hydrodynamical expansion. Let us develop this idea in detail.

5.2 Equation of State.

The hadron pressure is given in the statistical model by

$$P \;=\; \sum_i \frac{g_i}{2\pi^2\hbar^3} \int_0^\infty p^2 dp \; \frac{p^2}{3(p^2+m_i^2)^{1/2}} \; f_i \; . \qquad (4)$$

Using Eq. (4) we find that the equation of state, $P(\varepsilon)$, of the hadronic matter in the central region of Au+Au collisions at 10.7 AGeV is nearly linear with

ε. In fact, $P(\varepsilon)/\varepsilon$ is constant for the whole time interval t=10–18 fm/c

$$P/\varepsilon \;\cong\; 0.12\;. \tag{5}$$

This constant corresponds to the square of the speed of sound in the medium, $c_s^2 = (dP/d\varepsilon) \cong 0.12$, which is very similar to that in a resonance gas, $c_s^2 \cong 0.14$, obtained in [4]. The constant behaviour of $P(\varepsilon)/\varepsilon$ confirms that transport models like UrQMD and RQMD do not predict any phase transition which would be manifest in the softest point of the EoS, $P(\varepsilon)/\varepsilon$ [11].

In Fig. 6 we compare the ideal gas pressure Eq. (4) with longitudinal, $P^{mic}_{\{z\}}$, and transverse, $P^{mic}_{\{x,y\}}$, pressures obtained in UrQMD as [31,32]:

$$P^{mic}_{\{x,y,z\}} \;= \sum_h \frac{p^2_{h\{x,y,z\}}}{3V(m_h^2 \;+\; p_h^2)^{1/2}}\;, \tag{6}$$

where V is volume of the cell, p_h represents the particle momentum and the sum in Eq. (6) is taken over all hadrons h in the cell. Fig. 6 shows a strong difference between $P^{mic}_{\{z\}}$ and $P^{mic}_{\{x,y\}}$ for t <10 fm/c. That this is due to the longitudinal flow in the cell at early times can be seen from the dashed curve, obtained for a cell with a shortened longitudinal side, $\Delta z < 1$ fm. The difference between $P_\perp$ and $P_\parallel$ vanishes already at t =6 fm/c, but at so early times there is still no equilibrium in the cell: the slopes of the energy spectra are quite different for different particle species. Only at $t \cong$10 fm/c the hadronic matter in the cell becomes equilibrated. At this time the microscopic pressure Eq.(6) in both cells also becomes nearly isotropic and approximately equal to the ideal gas one Eq.(4), $3P^{mic}_{\{z\}} \cong 3P^{mic}_{\{x,y\}} \cong P$. The strong anisotropy of the transverse and the longitudinal components of the pressure is also observed in three-fluid hydrodynamical model for the initial stages of central Au+Au collisions at AGS [33]. This finding is in stark contrast to the one-fluid hydrodynamical model, where the pressure is assumed to be locally isotropic at all times.

Corse graining problems inhibit the direct microscopic calculations of the entropy. However, the entropy density s can be calculated from the ideal gas model (using the microscopic ε, ρ_B, ρ_S as input, see above) by the thermodynamical identity

$$\varepsilon = Ts + \mu_B\rho_B + \mu_S\rho_S - P.$$

The strange particle contribution is negligibly small ($\mu_S\rho_S \approx 1$ MeV maximally) in comparison to the other terms which are of order 100 MeV. The entropy per baryon in the cell is nearly constant and is equal to

$$S/A = s/\rho_B \;\cong\; 12\;. \tag{7}$$

Hence, the time evolution of the cell is nearly isentropic for times t=10–18 fm/c and, therefore, similar to an ideal hydrodynamic expansion.

5.3 Comparison with infinite equilibrated matter.

Quantum statistical effects in the ideal hadron gas are small for the temperatures and chemical potentials, T and μ, from the Table 1. Bose statistics gives the strongest effect for the pions – the Bose pion number density at T= 100–150 MeV is about 10% larger than the Boltzmann approximation. The quantum statistical effects are only 1-2% for other hadrons.

To make a conclusion about LTE in heavy ion collisions in a given microscopic model one has to perform a comparison not only to the Statistical Model, but also to an equilibrated infinite matter system within the same microscopic model. The energy spectra and the particle yields in the central cell of Au+Au collisions were compared to the equilibrated hadronic matter calculations obtained in a box with periodic boundary conditions by employing the UrQMD model to such a closed system with the approximate microcanonical infinite matter. This closed box calculations must clearly be distinguished from the open system, off equilibrium, in the central cell of heavy ion collisions discussed before. The particle yields and energy spectra predicted in the UrQMD box calculations [34] for each set of ε, ρ_B and ρ_S values taken from Table 1 for the different time steps are in a good agreement with the UrQMD predictions in the central cell of Au+Au collisions (see Fig. 4). This additionally confirms that at the intermediate stage of the reaction t =10–18 fm/c the hadronic matter in the cell is in thermodynamical equilibrium. This also means that the closed box calculations (as well as SM) can be used to describe - of course not to predict - the time evolution of locally equilibrated open system of the heavy ion collisions discussed above.

The static box values agree approximately with the ideal gas hadron model. However, there are enhancements of the low-energy pion yields as compared to the ideal gas results observed in both the UrQMD cell- and the box- calculations, seen in Fig. 4. The box calculations [34], at $\rho_B = \rho_0$, show that this enhancement becomes even stronger with increasing energy density. This enhancement is due to the violation of the detailed balance conditions for string- and many-body resonance decays in microscopic models like UrQMD [34]. The additional pion production from many-body decay channels acts like a positive pion chemical potential. The Bose enhancement of pions should therefore be more pronounced at higher energy densities [35].

6 Conclusions.

Equilibration of hadronic matter produced in the central cell of Au+Au collisions at 10.7 AGeV has been studied in the microscopic UrQMD model. It is found that

- There are large deviations from thermal equilibrium for the high density phase, t <10 fm/c.
- Local thermal and chemical equilibration seems to set in, in the central cell, for the expansion stage, t=10–18 fm/c.
- Both the different particle yields and the energy spectra in the central cell change drastically with time. Still, their instantaneous values agree, separately, for different time steps $t \geq$10 fm/c, with correspondingly adjusted ideal hadron gas model values.
- The temperatures and baryonic densities extracted in the central cell drop rapidly from T =150 to 100 MeV and from $\rho_B = 2\rho_0$ to $0.3\rho_0$ for t =10 to 18 fm/c.
- The entropy per baryon is nearly constant, $S/A = s/\rho_B \cong 12$, during the time interval t =10–18 fm/c.
- The equation of state of this complex mixture of different particle "fluids" has a very simple form $P(\varepsilon) \cong 0.12\varepsilon$ for this range of T, ρ_B, ρ_S-values.
- A substantial enhancement of low-energy pions is observed in the UrQMD calculations as compared to the ideal gas results. This effect increases at higher energy densities due to the string- and many-body decays of the resonances.
- At t=10–18 fm/c the spectra and hadron multiplicities in the central reaction cell are in agreement with those found for equilibrated infinite matter in UrQMD calculations in a box with periodic boundary conditions. The time scale of the thermal and chemical equilibration is, however, much shorter in the present calculations for nuclear reactions in the cell than in the UrQMD box calculations. It is the short-lived pre-equilibrium high density initial phase which prepares the extreme entropy densities forming doorway state to the quasi-isentropic expansion for $t \geq$10 fm/c.

Let us stress again that these studies support a picture of strong deviation from *local* thermodynamical equilibration in the central cell for t <10 fm/c in A+A collisions at AGS energies. Large collective streaming-through flow is found even in the central cell at early times. The whole system never reaches *global* thermodynamical equilibrium. However, local equilibration is approached in central cell for the later times, $t \geq$10 fm/c. These flow effects are not large, however, at $t \geq$10 fm/c in the central cell, that is why it was chosen. The averaged squared velocities in the central cell at t=10 fm/c are $\langle (v_z^{flow})^2 \rangle \cong$ 0.04 and $\langle (v_{x,y}^{flow})^2 \rangle \cong$ 0.01 for all particle species. These values are much smaller than the thermal velocities of the various hadrons in the cell at that

time. For nucleons one finds $\langle v_{th}^2 \rangle \cong 3T/m_N \cong 0.5$. Thermal velocities for pions and kaons are even larger. Our analysis neglects this small collective motion inside the central cell at t=10–18 fm. More careful studies give corrections to this picture: in Fig. 4 one observes that the "best fits" to the particle spectra would give $T_{N,\Delta} > T_{\pi,K}$: small collective motion inside the cell can imitate slightly larger (several percents) effective temperatures for heavier particles in the ideal gas calculations. Much larger flow velocities are found for all cells other than the central one.

A similar analysis has been done at lower energies in [31,36,37]. The next step is to study the approach to LTE for the earlier phase of the evolution and at higher collision energies (from the AGS to the SPS). This requires much smaller cell sizes and correspondingly larger samples of A+A events.

7 Acknowledgements.

L.V.B. is grateful to L. Csernai, I.N. Mishustin, E. Shuryak, J. Vaagen and E.E. Zabrodin for fruitful discussions. M.I.G. is thankful to K.A. Bugaev and M. Gaździcki for useful comments. This work was supported by A. v. Humboldt Stiftung, DFG, BMBF, Graduiertenkolleg "Exp. u. Theoret. Schwerionenphysik" and J. Buchmann Stiftung.

References

[1] E. Fermi, Prog. Theor. Phys. 5 (1950) 570; Phys. Rev. 81 (1951) 683.

[2] I.Ja. Pomeranchuk, Doklady Akad. Nauk SSSR, 78 (1951) 889.

[3] L.D. Landau, Izv.Akad.Nauk SSSR 17 (1953) 51.

[4] E. Shuryak, Yadernaya Fiz. (Sov. J. of Nucl. Phys.) 16 (1972) 395.

[5] J. Hofmann, H. Stöcker, U. Heinz, W. Scheid, W. Greiner, Phys. Rev. Lett. 36 (1976) 88

[6] K. Geiger, Phys. Rep. 258 (1995) 237.

[7] U. Heinz, nucl-th/9801050, Nucl. Phys. A (1998), in press; E. Schnedermann, J. Sollfrank and U. Heinz, Phys. Rev. C48 (1993) 2462.

[8] J. Cleymans and H. Satz, Z. Phys. C57 (1993) 135; J. Cleymans, K. Redlich, H. Satz and E. Suhonen, Z. Phys. C58 (1993) 347.

[9] P. Braun-Munzinger, J. Stachel, J.P. Wessel and N. Xu, Phys. Lett. B344 (1995) 43; Phys. Lett. B365 (1995) 1; J. Stachel, Nucl. Phys. A610 (1996) 509c.

[10] G. D. Yen, M. I. Gorenstein, W. Greiner and S. N. Yang, Phys. Rev. C56 (1997) 2210.

[11] C.M. Hung and E. Shuryak, Phys. Rev. Lett. 75 (1995) 4003; Phys. Rev. C56 (1997) 453; hep-ph/9608299.

[12] S.A. Bass, C. Hartnack, H. Stöcker and W. Greiner, Phys. Rev. C 50 (1994) 2167; M. Bleicher et al, in Proceedings of the Winter Meeting in Nuclear Physics (1997), Bormio, nucl-th/9704065.

[13] L.V. Bravina, I.N. Mishustin, A.N. Amelin, J. Bondorf, L.P. Csernai, Phys. Lett. B354 (1995) 196; Heavy Ion Phys. 5 (1997) 455.

[14] H. Sorge, Phys. Lett. B373 (1996) 16.

[15] R. Mattiello, A. Jahns, H. Sorge, H. Stöcker and W. Greiner, Phys. Rev. Lett. 74 (1995) 2180;
R. Mattiello, H. Sorge, H. Stöcker and W. Greiner, Phys. Rev. C 55 (1997) 1443.

[16] S.A. Bass et al, Prog. Part. Nucl. Phys. 41 (1998), in press; nucl-th/9803035.

[17] N.S. Amelin *et al.*, Sov. J. Nucl. Phys. 51 (1990) 1093; 52 (1990) 172; N.S. Amelin, L.V. Bravina, L.P. Csernai, V.D. Toneev, K.K. Gudima and S.Yu. Sivoklokov, Phys. Rev. C47 (1993) 2299.

[18] H. Sorge, H. Stöcker and W. Greiner, Ann. of Phys. 192 (1989) 266

[19] Y. Pang, T.J. Schagel and S.H. Kahana, Phys. Rev. Lett. 68 (1992) 2743.

[20] Bao-An Li and Che Ming Ko, Phys.Rev. C52 (1995) 2037; Phys. Rev. C53 (1996) 22.

[21] A.A. Amsden, A.S. Goldhaber, F.H. Harlow, J.R. Nix, Phys. Rev. C17 (1978) 2080;
L.P. Csernai et al., Phys. Rev. C26 (1982) 149;
R.B. Clare, D. Strottman, Phys. Rep. 141 (1986) 177;
H.W. Barz, B. Kämpfer, L.P. Csernai, B. Lukacs, Nucl. Phys. A465 (1987) 743;
H.W. Barz, B. Kämpfer, Phys. Lett. B206 (1988) 399.

[22] S. Bernard, J. A. Maruhn, W. Greiner, D. H. Rischke, Nucl.Phys. A605 (1996) 566.

[23] B. R. Schlei, U. Ornik, M. Plumer, D. Strottman, R. M. Weiner, Phys. Lett. B376 (1996) 212; U.Ornik, F. Pottag, R.M. Weiner, Phys. Rev. Lett. 63 (1989) 2641.

[24] H. Stöcker and W. Greiner, Phys. Rep. 137 (1986) 277.

[25] S.A. Bass, et al, Phys. Rev. Lett. (1998) in press, nucl-th/9711032.

[26] F. Becattini, Z. Phys. C69 (1996) 485.

[27] H. Stöcker, A.A. Ogloblin and W. Greiner, Z. Phys. A303 (1981) 259.

[28] D. Hahn and H. Stöcker, Nucl. Phys. A476 (1988) 718.

[29] M. I. Gorenstein and S. N. Yang, Phys. Rev. C44 (1991) 2875; M. I. Gorenstein, H. G. Miller, R. M. Quick and S. N. Yang, Phys. Rev. C50 (1994) 2232; M. I. Gorenstein and H. G. Miller, Phys. Rev. C55 (1997) 2002.

[30] J. Cleymans, D. Elliot, H. Satz and R. L. Thews, Z. Phys. C 74 (1997) 319.

[31] M. Berenguer, C. Hartnack, G. Peilert, H. Söcker, W. Greiner, J. Aichelin and A. Rosenhauer, J. Phys. G 18 (1992) 655.

[32] H. Sorge, Phys. Rev. Lett. 78 (1997) 2309; Phys. Lett. B402 (1997) 251.

[33] J. Brachmann, A. Dumitru, J.A. Maruhn, H. Stöcker, W. Greiner, D.H. Rischke, Nucl. Phys. A619 (1997) 391; A. Dumitru, J. Brachmann, M. Bleicher, J.A. Maruhn, H. Stöcker, W. Greiner, Heavy Ion Phys. 5 (1997) 357.

[34] M. Belkacem et al., nucl-th/9804058, submitted for publication in Phys. Rev. C; M. Brandstetter et al., in preparation.

[35] I.N. Mishustin, L.M. Satarov, J. Maruhn, H. Stöcker, W. Greiner, Z. Phys. A342 (1992) 309.

[36] D. Bandyopadhyay, M. Gorenstein, H. Stoecker, W. Greiner, H. Sorge, Z. Phys. C58 (1993) 461.

[37] J. Konopka et al., Proceedings of CRIS'96, eds. S. Costa, S. Albergo, A. Insolia, C. Tuve, World Scientific, 1996, p.378, nucl-th/960715.

Table 1
The thermodynamic characteristics of the hadronic matter in the central cell (V=125 fm^3) in central Au+Au collisions at 10.7AGeV. The energy density, ε, baryonic density, ρ_B, and net strangeness density, ρ_S, are obtained from the microscopic UrQMD calculations. The temperature, T, baryonic chemical potential, μ_B, and strange chemical potential, μ_S, are extracted from the ideal hadron gas model, using ε, ρ_B and ρ_S as input.

t (fm)	ε (MeV/fm^3)	ρ_B (fm^{-3})	ρ_S (fm^{-3})	T (MeV)	μ_B (MeV)	μ_S (MeV)
10	675	0.33	-0.008	147	510	128
11	511	0.26	-0.007	140	519	122
12	384	0.20	-0.006	134	527	116
13	293	0.16	-0.004	128	534	112
14	222	0.12	-0.003	122	542	107
15	170	0.10	-0.003	116	553	101
16	134	0.08	-0.003	111	560	96
17	102	0.06	-0.003	106	567	87
18	80	0.05	-0.002	101	574	79

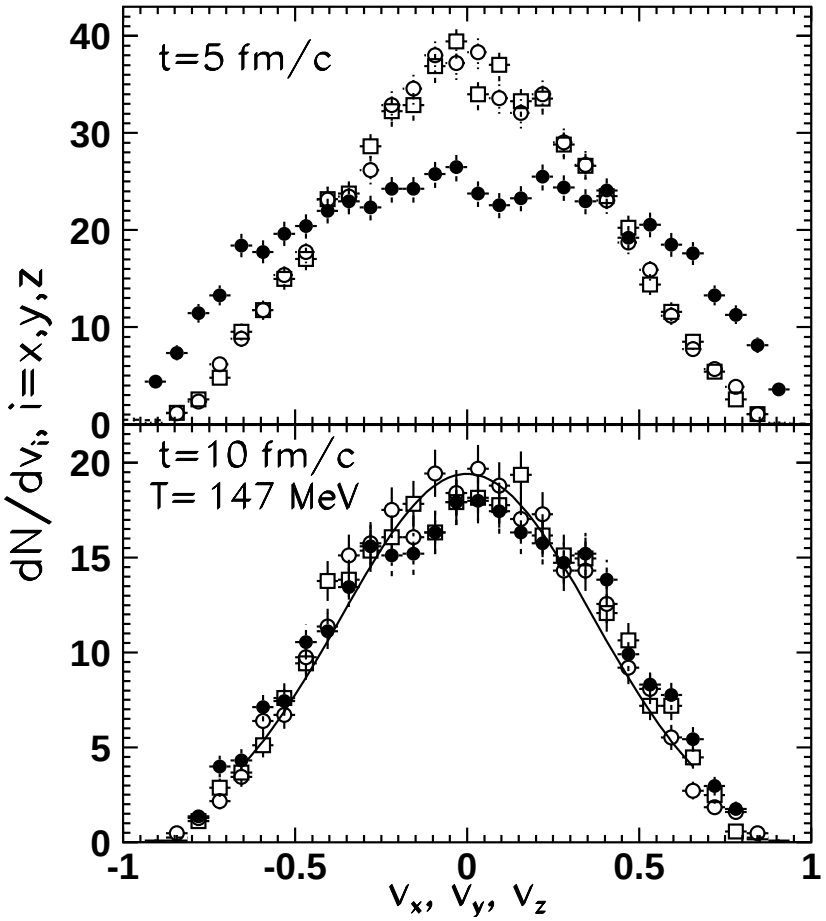

Fig. 1. Nucleon velocity distributions dN/dv_i ($i = z$ (•), x (□) and y (◯)) in central cell of Au+Au collisions at 10.7 AGeV at t =5 (upper frame) and 10 (lower frame) fm/c. The solid line corresponds to the Maxwell-Boltzmann velocity distribution $dN/dv_i \sim \exp(-m_N v_i^2/2T)$ for the "non-relativistic" ($v_i < 0.6$) nucleons with temperature $T = 147$ MeV as obtained in ideal gas model.

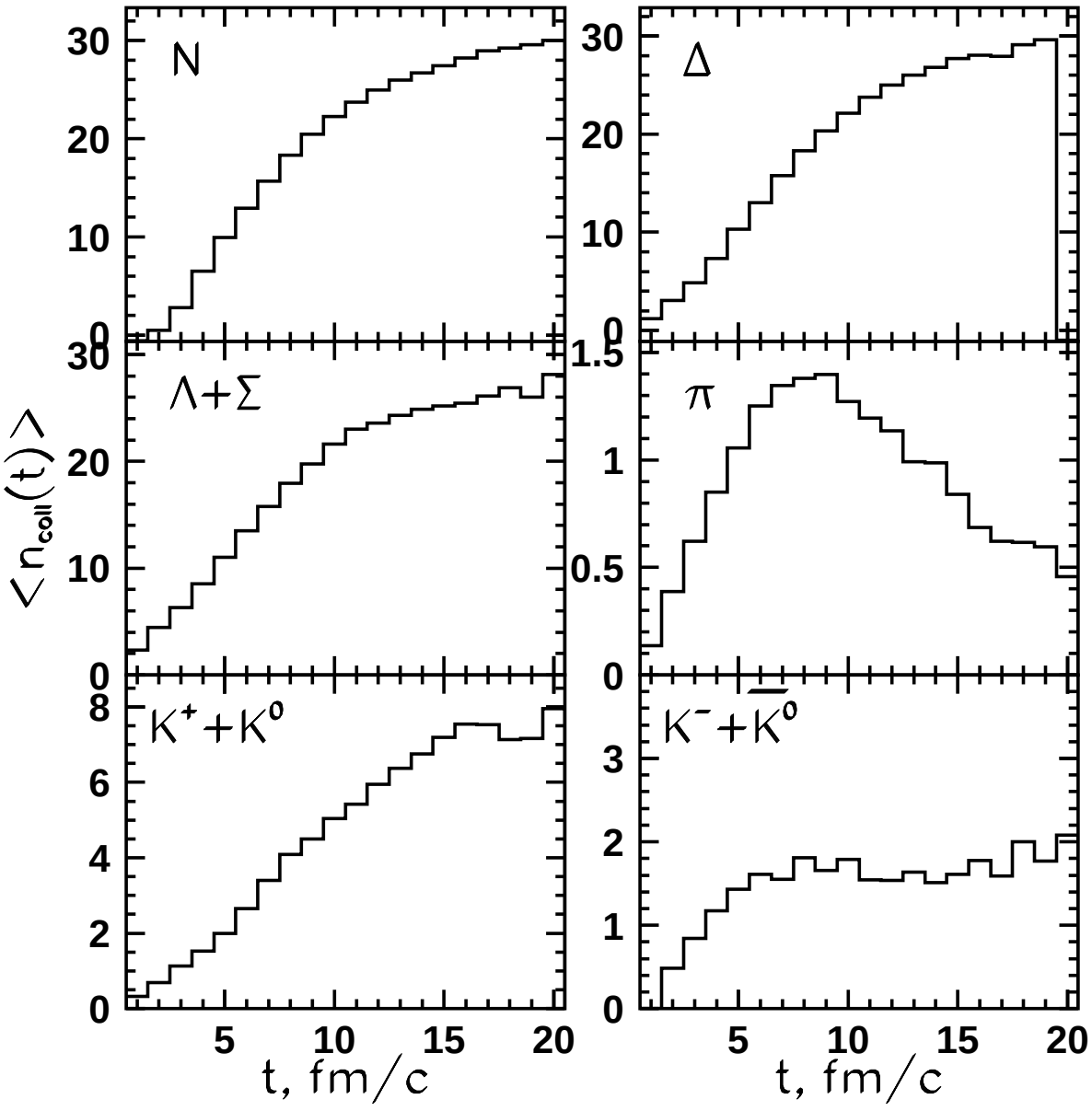

Fig. 2. The number of collisions, $< n_{coll}(t) >$, in the central cell of Au+Au collisions at 10.7 AGeV versus time, t, for nucleons, deltas, lambdas plus sigmas, pions, kaons and antikaons.

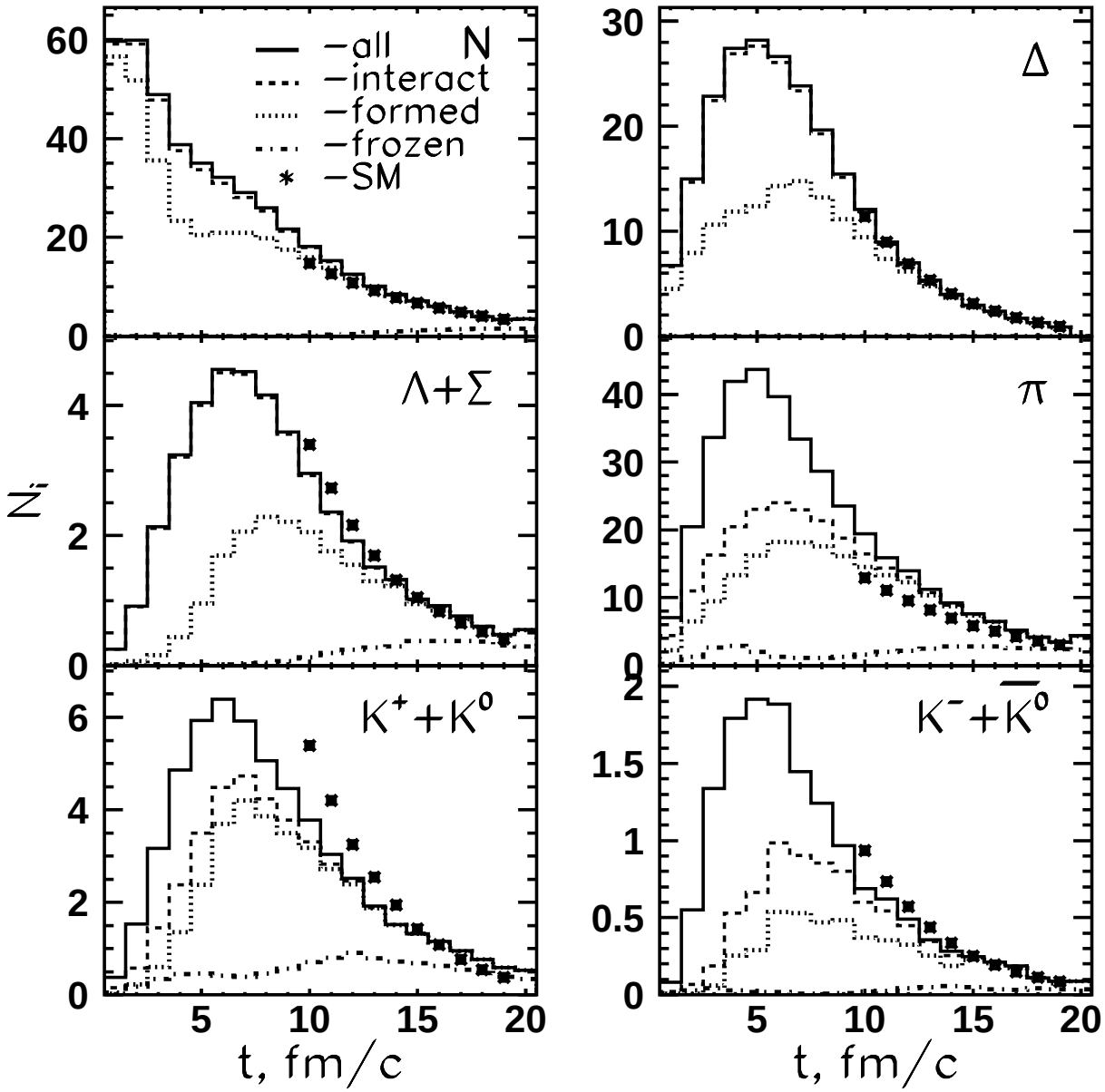

Fig. 3. The number of particles in the central cell of Au+Au collisions at 10.7 AGeV as a function of time as obtained in UrQMD model (histograms). Solid lines correspond to all hadrons in the cell, dashed lines – to interacting particles and dotted lines – to formed hadrons. The numbers of frozen particles in the cell are shown by dot-dashed lines. The points represent the predictions of the ideal gas model as calculated at the same energy, baryonic and strangeness densities as for the UrQMD central cell.

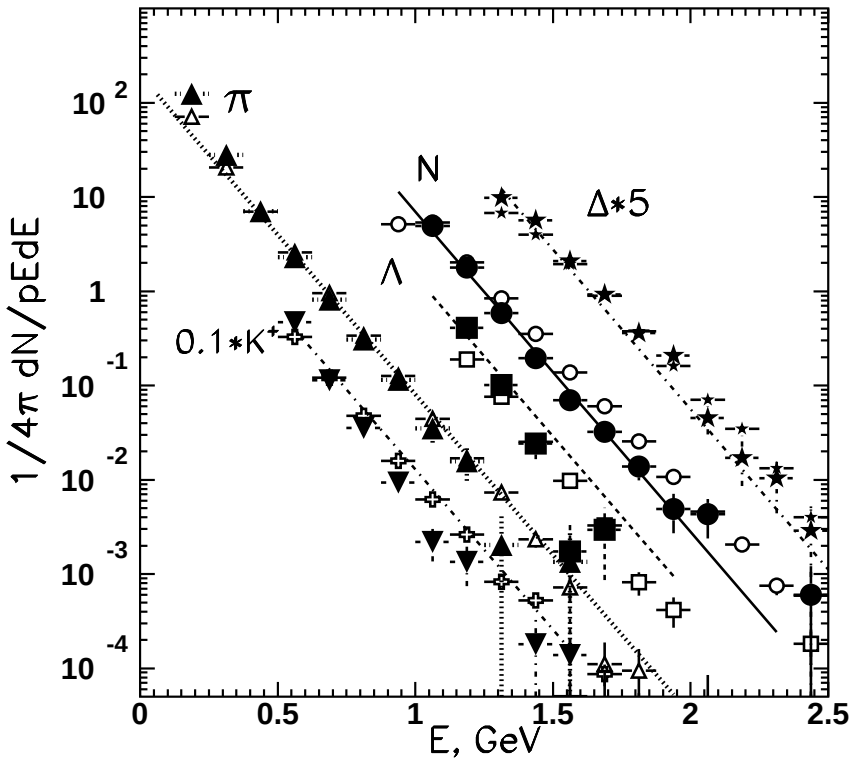

Fig. 4. Energy spectra of N ($\bullet$), Λ ($\square$), π ($\triangle$), K^+ ($\bigtriangledown$) and Δ ($\star$) in the central 125 fm^3 cell of Au+Au collisions at 10.7 A·GeV at t=13 fm/c (black points) and in box calculations (open points) are fitted by Boltzmann distributions, Eq. (1) (lines) using the parameters T=128 MeV, μ_B=534 MeV, μ_S = 112 MeV, as obtained in the ideal gas model.

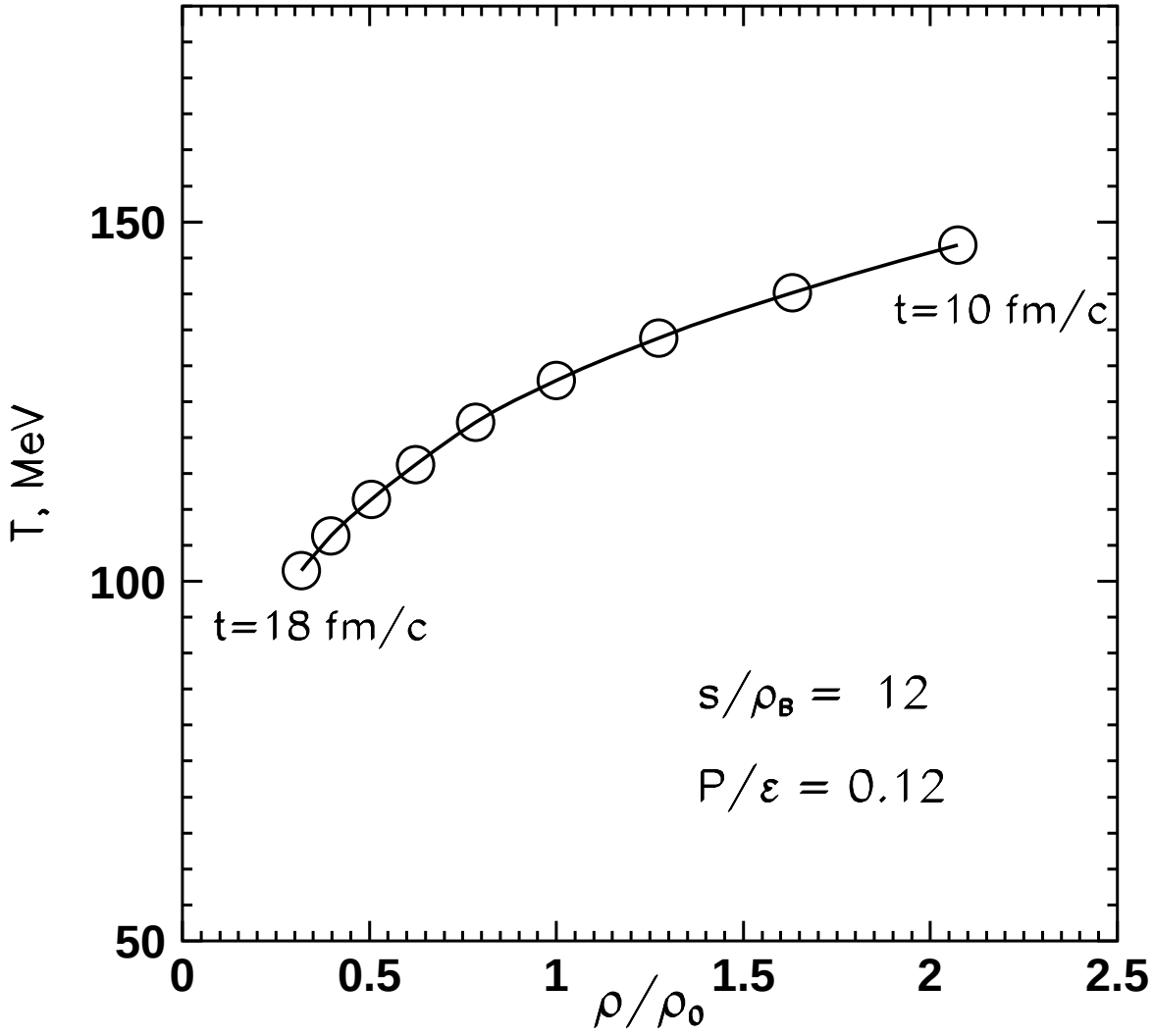

Fig. 5. The evolution of the baryon density, ρ_B, and temperature, T, in the central cell of Au+Au collisions at 10.7 AGeV at times t=10–18 fm/c. The entropy per baryon is constant $s/\rho_B \approx 12$ thus exhibiting quasi-isentropic expansion in this central cell. The equation of state has the form $P \approx 0.12\varepsilon$.

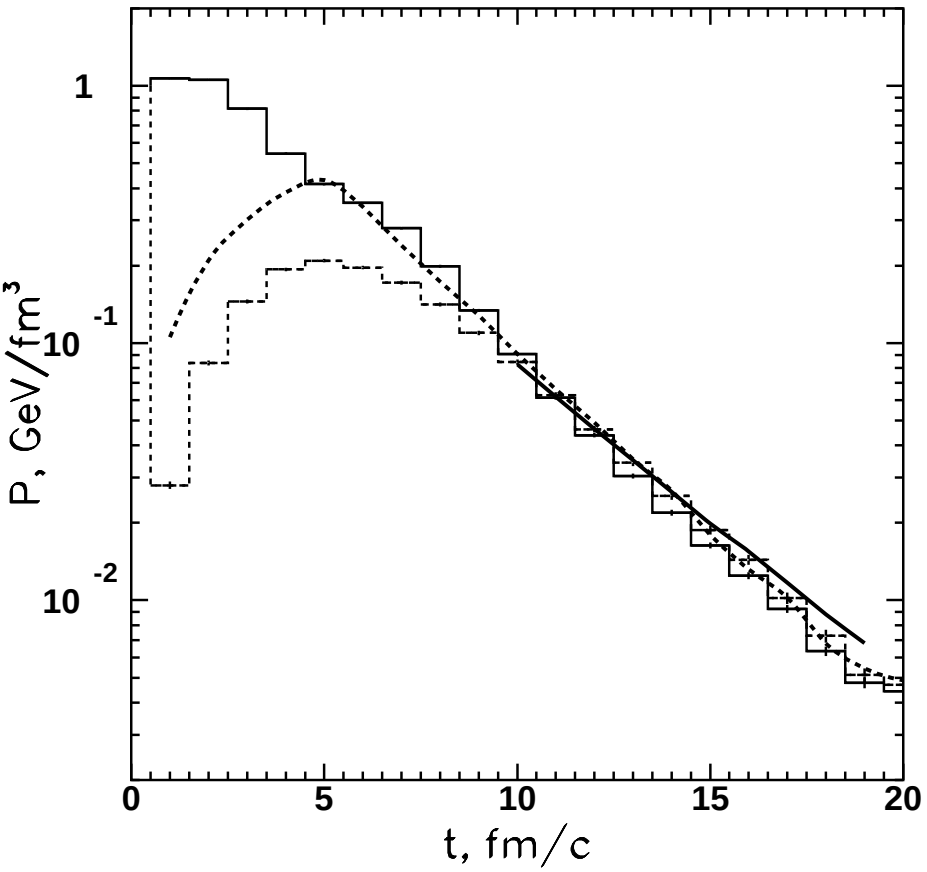

Fig. 6. The longitudinal ($3 \cdot P_{\{z\}}$, solid histogram) and the transverse ($3 \cdot P_{\{x,y\}}$, dashed curves) diagonal components of the microscopic pressure tensor in the central cell ($\Delta x \times \Delta y \times \Delta z = \ 5 \times 5 \times 5$ fm^3 (histograms) and $4 \times 4 \times 1$ fm^3, (dashed line)) of Au+Au collisions at 10.7 AGeV calculated from the virial theorem Eq. (6) are compared to the ideal gas pressure Eq. (4) (solid line).